

Article

## Model for Predicting DC Flashover Voltage of Pre-Contaminated and Ice-Covered Long Insulator Strings under Low Air Pressure

Jianlin Hu \*, Caixin Sun, Xingliang Jiang, Qing Yang, Zhijin Zhang and Lichun Shu

State Key Laboratory of Power Transmission Equipments & System Security and New Technology, College of Electrical Engineering, Chongqing University, Chongqing 400044, China; E-Mails: suncx@cqu.edu.cn (C.S.); jxl0731@126.com (X.J.); yangqing@cqu.edu.cn (Q.Y.); zhangzhijing@cqu.edu.cn (Z.Z.); lcsu@cqu.edu.cn (L.S.)

\* Author to whom correspondence should be addressed; E-Mail: hujianlin@cqu.edu.cn; Tel.: +86-23-65111172 (ext. 8219); Fax: +86-23-65102442.

Received: 28 February 2011; in revised form: 13 April 2011 / Accepted: 18 April 2011 / Published: 19 April 2011

---

**Abstract:** In the current study, a multi-arc predicting model for DC critical flashover voltage of iced and pre-contaminated long insulator strings under low atmospheric pressure is developed. The model is composed of a series of different polarity surface arcs, icicle-icicle air gap arcs, and residual layer resistance. The calculation method of the residual resistance of the ice layer under DC multi-arc condition is established. To validate the model, 7-unit and 15-unit insulator strings were tested in a multi-function artificial climate chamber under the coexistent conditions of low air pressure, pollution, and icing. The test results showed that the values calculated by the model satisfactorily agreed with those experimentally measured, with the errors within the range of 10%, validating the rationality of the model.

**Keywords:** ice-covered insulator string; flashover; mathematical model; DC; low air pressure; pre-contamination

---

## 1. Introduction

Ice accretion is a beautiful natural phenomenon. However, it can also be a serious natural disaster for insulators of overhead power transmission lines. In most cold regions of the world, overhead transmission lines and their substations are subject to ice accumulation each year for an extended period of time due to freezing rain or drizzle, in-cloud icing, icing fog, wet snow, or frost. One of the most challenging problems associated with ice and snow accretion on overhead transmission lines is the loss of electrical performance of the insulators. Under certain conditions, a drastic decrease in electrical insulation can lead to flashover and consequent power outages [1–12]. Depending on the weather conditions, different types of ice may accrete on an insulator surface. Among them, glaze accompanied with icicles grown in a wet regime is known as the one that is most likely to induce flashover on insulators [8–12].

Insulator flashover under glaze ice accretion has been reported from several countries and has received a great deal of attention from many researchers [8–19]. A large number of investigations and theoretical studies have been carried out in several laboratories [1–27]. These studies focus on two aspects: one is the flashover characteristics of ice-covered insulators, *i.e.*, carrying out artificial icing on insulators in an artificial climate chamber or outdoor station, evaluating the flashover characteristics of ice-covered insulators according to certain experimental procedures, and analyzing the effects of insulator types, insulator profiles, arrangement, dry arc distance, leakage distance, icing parameters, contamination degree, atmospheric condition, and voltage type on flashover/withstand voltage; the other is the predicting model for flashover voltage of ice-covered insulators, *i.e.*, analyzing the development characteristics of the arc, arc parameters, and electrical field during the flashover process of ice-covered insulators and building the physical-mathematical model for calculating the flashover voltage of ice-covered insulators.

As far as models for predicting the flashover voltage of ice-covered insulators are concerned, both static [21–23] and dynamic [24–26] mathematical models have been developed to simulate flashover on insulators. Static models are based on the Obenaus Serial Circuit Model. The flashover on an ice surface is considered an arc in series with a residual resistance consisting of an ice layer not bridged by the arc. Based on arc constants, surface conductance, and reignition conditions obtained from experiments as well as on the simultaneous solutions of serial circuit equations, the characteristics of the arc at its critical length leading to flashover and residual ice layer resistance can be obtained. The model can be used to predict the critical arc length and the critical flashover voltage of ice-covered insulators. The model has been successfully applied to short insulator strings covered with wet grown ice [21–23]. The effects of such parameters as insulator diameter and atmospheric pressure on the flashover voltage of ice-covered insulators have been studied using this model [21]. In contrast, the dynamic model adopts a dynamic approach based on the physical processes constituting the phenomena. In the dynamic model, the arc is considered a time-dependent impedance, and the flashover process is simulated in steps. This model can be used to predict the arc velocity, flashover time, critical flashover voltage, and leakage current during the flashover process [24]. Nowadays, the static and dynamic models for short string ice-covered insulators are being successfully developed. However, compared with those for long string ice-covered insulators, the present models need further improvements. Farzaneh and Zhang built an AC multi-arc predicting model for long string

ice-covered insulators based on the static icing models [23]. The predicting model is in accordance with the test results, but it cannot be directly applied to the condition of multi arcs in the discharge process of DC long string ice-covered insulators due to the arc polarity effects. In addition, there is no discharge model for DC long string insulators under the combined conditions of high altitude, icing, and contamination.

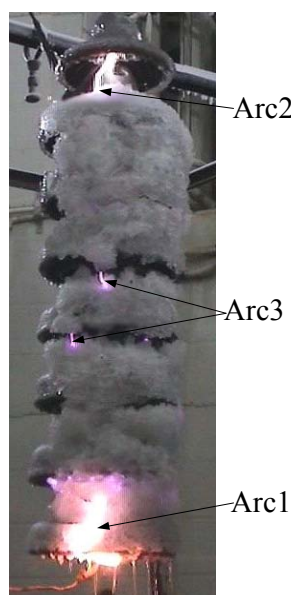
Currently, many Ultra High Voltage (UHV) DC transmission lines are being constructed and operated in China, most of which need to cross regions of high altitude, pollution, and icing, yet the external insulation discharge characteristic under the coexistent conditions of high altitude, pollution, and icing is an unsolved problem. The problem is crucial to the construction of the UHV power transmission and the development of power grids. The main purposes of the current paper are to summarize the static model and to expand the static model to a validated multi-arc model for predicting the DC flashover voltage of ice-covered insulators used in the power networks of voltage levels up to UHV. Power grids in the future tend to be intelligentized, with equipment condition assessment as its crucial part. Thus, the development of such a model can lay the foundation for assessing the outer insulation state of transmission lines in power grids in the future.

## 2. Model for Predicting the DC Flashover Voltage of Pre-Polluted and Ice-Covered Long Insulator Strings under Low Air Pressure

### 2.1. Multi-Arc Model for DC Flashover of Ice-Covered Insulators

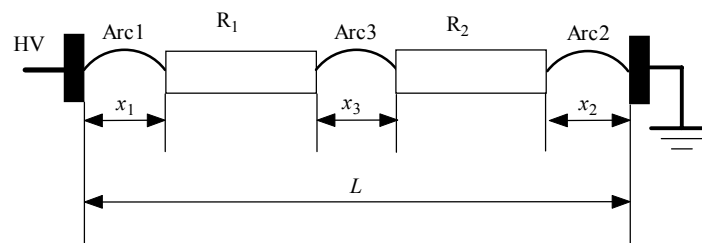
Similar to the discharge process of long string AC ice-covered insulators described in literature [23], partial arcs can possibly occur at the high voltage end, the ground end, or between the icicles in the middle part of the insulator string. In addition, the coexistence of arcs at several sites and their development until a complete flashover can also occur. As shown in Figure1, the arcs develop at both the high voltage end and the ground end during the DC flashover process of 7-unit XZP-210 insulator strings.

**Figure 1.** Multi-arc on ice-covered insulators during the DC flashover process.



Two arcs occur in the icicle-icicle air gaps. With the increase in length of the ice-covered insulator strings, there is a greater possibility for the co-development of arcs at different sites [25]. According to multi-arc models for AC long string ice-covered insulators in literature [23], the equivalent serial circuit model in Figure 2 can be applied if there is an arc development at both the high voltage end and the ground end, and if one arc occurs at the icicle-icicle air gap during the DC discharge process of ice-covered insulators. In Figure 2, Arc1 refers to the surface arc developing from the high voltage end with an arc length  $x_1$ , Arc2 is the surface arc developing from the ground end with an arc length  $x_2$ , Arc3 is the air gap arc developing from the icicle-icicle air gap in the middle part of the insulator string with an arc length  $x_3$ , and both  $R_1$  and  $R_2$  are the residual resistances of the ice layer unbridged by the arcs.

**Figure 2.** Model of the three arcs.



According to the classical statistic discharge model for ice-covered insulators [21–23], the applied voltage is the sum of multiple arc voltage drops and multiple residual resistance voltages under a steady arc burning condition, *i.e.*:

$$U = U_{\text{arc1}} + U_{e1} + U_{\text{arc2}} + U_{e2} + U_{\text{arc3}} + U_R \quad (1)$$

where  $U$  is the applied voltage,  $U_{\text{arc1}}$  the arc voltage drop at the high voltage end,  $U_{e1}$  the electrode voltage drop at the high voltage end,  $U_{\text{arc2}}$  the arc voltage drop at the ground end,  $U_{e2}$  the electrode voltage drop at the ground end,  $U_{\text{arc3}}$  the arc voltage drop at the icicle-icicle air gap whose positive and negative voltage drops can be ignored due to the lack of electrode at both ends, and  $U_R$  the sum of the voltage of each residual resistance.

According to arc theory, under the DC condition, if the applied voltage at the high voltage end is positive, the arc developing from that end is positive, whereas the arc developing from the ground end is negative. If the applied voltage at the high voltage end is negative, the arc developing from that end is negative, but the arc developing from the ground end is positive. Therefore, arcs of ice-covered insulators can be classified as positive surface arc, negative surface arc, and icicle-icicle air gap arc in the flashover process of long string DC insulator strings. Studies so far indicate that these three types of arcs have different voltage-current characteristics [27–30]. Thus, the sum of the length of the three arcs in Figure 2 cannot represent the total arc voltage.

Suppose:

$$\begin{cases} x_1 = a_1 x \\ x_2 = a_2 x \\ x_3 = a_3 x \end{cases} \quad (2)$$

where  $a_1$ ,  $a_2$ , and  $a_3$  are the proportions of arc length at the high voltage end, arc length at the ground end, and arc length of icicle-icicle air gap arc to the total arc length respectively, and  $x$  is the total arc length, *i.e.*:

$$x = x_1 + x_2 + x_2 \tag{3}$$

Arcs usually float during the flashover process of ice-covered DC insulators. With the decrease in the atmospheric pressure and the increase in salt deposit density,  $\text{mg}/\text{cm}^2$  (*SDD*), arc floating becomes more serious [27]. Due to the occurrence of arc floating, both the arc length and the arc voltage change accordingly. In the flashover models for ice-covered insulators, arc length is presumed to be equal to the distance along the ice surface considering arc floating. The arc floating coefficient  $k$  is used to calculate the change in the arc length caused by the floating arc, with values in the range of 1.2–1.4 [20–22,29].

Under low air pressure conditions, the surface arc characteristics of ice-covered insulators also change [27–30]. The following formula can be used to express the surface arc characteristics of ice-covered insulators affected by the atmospheric pressure [28,30]:

$$\begin{cases} U_{\text{arc}} = A\left(\frac{P}{P_0}\right)^m xI^{-n} \\ U_e = B\left(\frac{P}{P_0}\right)^e \end{cases} \tag{4}$$

where  $P$  is the experimental conditional atmospheric pressure, in kPa;  $P_0$  is the standard atmospheric pressure, in kPa;  $I$  is the leakage current, in A;  $m$  and  $e$  are the exponents characterizing the atmospheric pressure influence;  $A$  and  $n$  are the arc constants;  $B$  is the electrode voltage drop constant.

Therefore, taking into account the arc floating and arc characteristics under low air pressure,  $U_{\text{arc1}}$ ,  $U_{\text{arc2}}$ , and  $U_{\text{arc3}}$  in Equation (1) can be expressed as:

$$\begin{cases} U_{\text{arc1}} = A_1\left(\frac{P}{P_0}\right)^{m_1} kx_1I^{-n_1} = A_1\left(\frac{P}{P_0}\right)^{m_1} k_1a_1xI^{-n_1} \\ U_{\text{arc2}} = A_2\left(\frac{P}{P_0}\right)^{m_2} kx_2I^{-n_2} = A_2\left(\frac{P}{P_0}\right)^{m_2} k_2a_2xI^{-n_2} \\ U_{\text{arc3}} = A_3\left(\frac{P}{P_0}\right)^{m_3} kx_3I^{-n_3} = A_3\left(\frac{P}{P_0}\right)^{m_3} k_3a_3xI^{-n_3} \end{cases} \tag{5}$$

The values for the arc electrode voltage drops  $U_{e1}$  and  $U_{e2}$  are as follows:

$$\begin{cases} U_{e1} = B_1\left(\frac{P}{P_0}\right)^{e_1} \\ U_{e2} = B_2\left(\frac{P}{P_0}\right)^{e_2} \end{cases} \tag{6}$$

The total voltage of the residual resistance  $U_R$  is:

$$U_R = IR(x) \tag{7}$$

By substituting Equations (5)–(7) into Equation (1), the expression for the applied voltage needed to maintain the steady development of the three arcs during the DC discharge of ice-covered insulators under low atmospheric pressure can be obtained and is shown as follows:

$$U = A_1 \left(\frac{P}{P_0}\right)^{m_1} k a_1 x I^{-n_1} + B_1 \left(\frac{P}{P_0}\right)^{e_1} + A_2 \left(\frac{P}{P_0}\right)^{m_2} k a_2 x I^{-n_2} + B_2 \left(\frac{P}{P_0}\right)^{e_2} + A_3 \left(\frac{P}{P_0}\right)^{m_3} k a_3 x I^{-n_3} + IR(x) \tag{8}$$

If the arc polarity effects of the icicle-icicle air gap arc are ignored, all the icicle-icicle air gap arcs can be counted as one arc in the middle, regardless of the number of icicle-icicle air gap arcs occurring in the middle part of the insulator strings. Thus, Equation (8) can also be applied to cases where there is a random number of arcs among the insulator strings.

2.2. Residual Resistance of Ice Layer under DC Multi-Arc Condition

According to Equation (8), the calculation method for the residual resistance of the ice layer for different arc lengths is indispensable to the calculation of the DC critical flashover voltage of ice-covered insulator strings. Based on the calculating method for the residual resistance under the pollution condition proposed by Wilkins [31], scholars such as Farzaneh [21–22] argued that under the single arc condition, as shown in Figure 3, the residual resistance cannot be directly replaced by the physical resistance due to the current convergence effects on the arc root. They have deduced the expression for calculating the residual resistance of the ice layer where half of the cylinder is covered with ice, shown as follows:

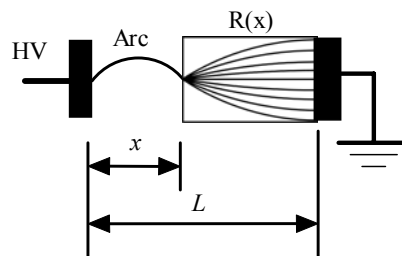
$$R(x) = \frac{1}{2\pi\gamma_e} \left[ \frac{4(L-x)}{D+2d} + \ln\left(\frac{D+2d}{4r_a}\right) \right] \tag{9}$$

where  $D$  is the insulator radius,  $d$  is the ice thickness,  $\gamma_e$  is the equivalent conductivity of the residual ice layer,  $L$  is the flashover distance of the ice-covered insulator string,  $x$  is the arc length, and  $r_a$  is the arc radius. The change in the arc radius  $r_a$  accompanying the change in the current can be expressed as:

$$r_a = \sqrt{\frac{I}{\pi J}} \tag{10}$$

where  $J$  is the current density.

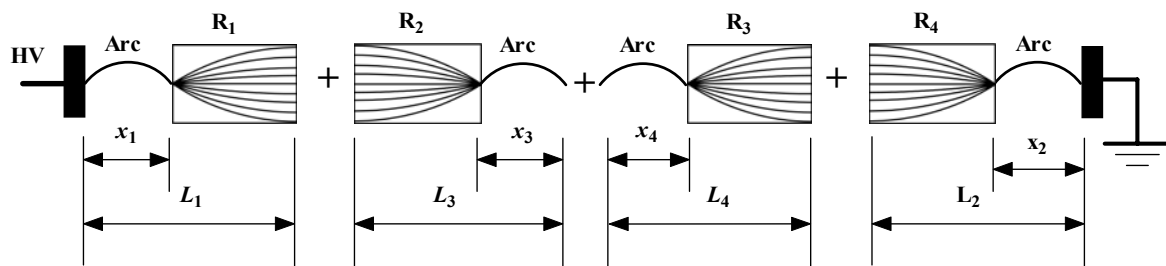
Figure 3. Residual resistance calculation model of a single arc.



In cases where there are long string insulators with multi-arcs, the distribution of leakage currents changes on the surface of ice-covered insulators because of the existence of multi-arcs and the current convergence effects on the arc root. As shown in Figure 2, the surface currents of the residual resistance converge at the two ends of the three arcs. Therefore, the total residual ice layer resistance cannot be calculated by simply adding up all the arc lengths according to Equation (9).

For example, when one surface arc exists at the high voltage end, the ground end, and the icicle-icicle air gap arc in the middle, respectively, the calculating method for the residual resistance under the multi-arc condition is explored. Every residual resistance in Figure 2 is divided from the middle, and the icicle-icicle air gap arc is halved to gain the series circuit, as shown in Figure 4. In Figure 4, there is only one end directly connected to the arc with the current convergence at the arc root after dividing each resistance. Thus, Equation (9) can be used to calculate each residual resistance after the division.

**Figure 4.** Equivalent single-arc residual resistance calculation model for three arcs.



Each residual resistance can be shown as follows:

$$R_1 = \frac{1}{2\pi\gamma_e} \left[ \frac{4(L_1 - x_1)}{D + 2d} + \ln\left(\frac{D + 2d}{4r_a}\right) \right] \tag{11}$$

$$R_2 = \frac{1}{2\pi\gamma_e} \left[ \frac{4(L_2 - x_2)}{D + 2d} + \ln\left(\frac{D + 2d}{4r_a}\right) \right] \tag{12}$$

$$R_3 = \frac{1}{2\pi\gamma_e} \left[ \frac{4(L_3 - x_3)}{D + 2d} + \ln\left(\frac{D + 2d}{4r_a}\right) \right] \tag{13}$$

$$R_4 = \frac{1}{2\pi\gamma_e} \left[ \frac{4(L_4 - x_4)}{D + 2d} + \ln\left(\frac{D + 2d}{4r_a}\right) \right] \tag{14}$$

In Equations (11)–(14),  $L_1$ ,  $L_2$ ,  $L_3$ , and  $L_4$  are the discharge distances, and  $x_1$ ,  $x_2$ ,  $x_3$ , and  $x_4$  are the arc lengths of each part of the three arcs after the division.

Total discharge distance  $L$  is given by:

$$L = L_1 + L_2 + L_3 + L_4 \tag{15}$$

Total arc length  $x$  is given by:

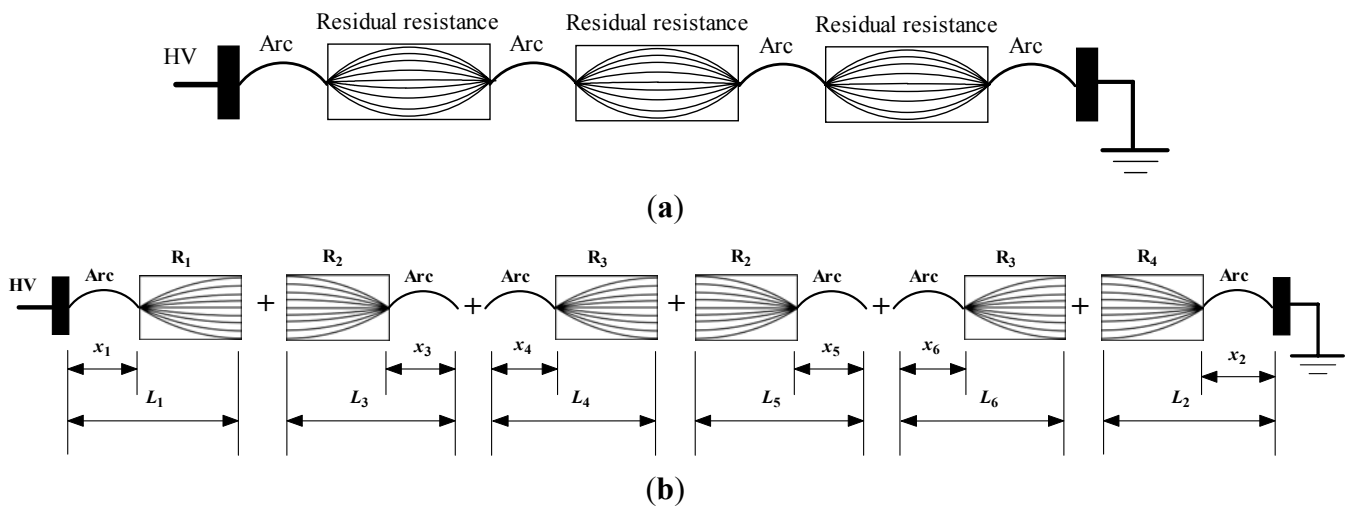
$$x = x_1 + x_2 + x_3 + x_4 \tag{16}$$

Therefore, when one surface arc exists at the high voltage end and the ground end, and when one arc is at icicle-icicle air gap in the middle part, the total residual ice layer resistance  $R$  can be shown as:

$$\begin{aligned} R &= R_1 + R_2 + R_3 + R_4 \\ &= \frac{1}{2\pi\gamma_e} \left[ \frac{4((L_1 + L_2 + L_3 + L_4) - (x_1 + x_2 + x_3 + x_4))}{D + 2d} + 4\ln\left(\frac{D + 2d}{4r_a}\right) \right] \\ &= \frac{1}{2\pi\gamma_e} \left[ \frac{4(L - x)}{D + 2d} + 4\ln\left(\frac{D + 2d}{4r_a}\right) \right] \end{aligned} \tag{17}$$

When one surface arc exists at the high voltage and the ground end, and when two icicle-icicle air gap arcs are in the middle of the insulators, the three residual resistances can also be divided into six parts, as shown in Figure 5(a). The two icicle-icicle air gap arcs can be divided into four parts, as shown in Figure 5(b).

**Figure 5.** Equivalent single-arc residual resistance calculation model for four arcs. (a) Schematic for the two icicle-icicle air gap arcs in the middle; (b) Schematic for the division of the arc in the middle.



Based on Figure 5, the total residual resistance  $R$  can be expressed as follows:

$$R = R_1 + R_2 + R_3 + R_4 + R_5 + R_6 \tag{18}$$

where:

$$R_1 = \frac{1}{2\pi\gamma_e} \left[ \frac{4(L_1 - x_1)}{D + 2d} + \ln\left(\frac{D + 2d}{4r_a}\right) \right] \tag{19}$$

$$R_2 = \frac{1}{2\pi\gamma_e} \left[ \frac{4(L_2 - x_2)}{D + 2d} + \ln\left(\frac{D + 2d}{4r_a}\right) \right] \tag{20}$$

$$R_3 = \frac{1}{2\pi\gamma_e} \left[ \frac{4(L_3 - x_3)}{D + 2d} + \ln\left(\frac{D + 2d}{4r_a}\right) \right] \tag{21}$$

$$R_4 = \frac{1}{2\pi\gamma_e} \left[ \frac{4(L_4 - x_4)}{D + 2d} + \ln\left(\frac{D + 2d}{4r_a}\right) \right] \tag{22}$$

$$R_5 = \frac{1}{2\pi\gamma_e} \left[ \frac{4(L_5 - x_5)}{D + 2d} + \ln\left(\frac{D + 2d}{4r_a}\right) \right] \tag{23}$$

$$R_6 = \frac{1}{2\pi\gamma_e} \left[ \frac{4(L_6 - x_6)}{D + 2d} + \ln\left(\frac{D + 2d}{4r_a}\right) \right] \tag{24}$$

By substituting Equations (19)–(24) into Equation (18), the following can be obtained:

$$R = \frac{1}{2\pi\gamma_e} \left[ \frac{4((L_1 + L_2 + L_3 + L_4 + L_5 + L_6) - (x_1 + x_2 + x_3 + x_4 + x_5 + x_6))}{D + 2d} + 4 \ln\left(\frac{D + 2d}{4r_a}\right) \right] \tag{25}$$

The total discharge distance  $L$  is:

$$L = L_1 + L_2 + L_3 + L_4 + L_5 + L_6 \quad (26)$$

The total arc distance  $x$  is:

$$x = x_1 + x_2 + x_3 + x_4 + x_5 + x_6 \quad (27)$$

With the two arcs at the high voltage end, the ground end, and the icicle-icicle air gap, the residual resistance can be shown as:

$$R(x) = \frac{1}{2\pi\gamma_e} \left[ \frac{4(L-x)}{D+2d} + 6 \ln\left(\frac{D+2d}{4r_a}\right) \right] \quad (28)$$

Similarly, when there is one arc at the high voltage end and the ground end, and when there is  $c$  ( $c \geq 0$ ) number of arcs in the icicle-icicle air gaps, the residual resistance is expressed as:

$$R(x) = \frac{1}{2\pi\gamma_e} \left[ \frac{4(L-x)}{D+2d} + (2c+2) \ln\left(\frac{D+2d}{4r_a}\right) \right] \quad (29)$$

Based on the analysis above, when there is one arc at the high voltage end,  $c$  ( $c \geq 0$ ) number of arcs in the icicle-icicle air gaps, and no arc at the ground end or when there is no arc at the high voltage end,  $c$  ( $c \geq 0$ ) number of arcs in the icicle-icicle air gaps, and one arc at the ground end, the residual resistance is shown as:

$$R(x) = \frac{1}{2\pi\gamma_e} \left[ \frac{4(L-x)}{D+2d} + (2c+1) \ln\left(\frac{D+2d}{4r_a}\right) \right] \quad (30)$$

When there is no arc at both the high voltage and ground ends, and when there is  $c$  ( $c \geq 0$ ) number of arcs in the icicle-icicle air gaps, the residual resistance is:

$$R(x) = \frac{1}{2\pi\gamma_e} \left[ \frac{4(L-x)}{D+2d} + 2c \ln\left(\frac{D+2d}{4r_a}\right) \right] \quad (31)$$

### 3. Validation of the Model

Based on the multi-arc discharge model for DC ice-covered insulators in the current study, the DC discharge voltage of the pre-contaminated ice-covered insulator strings under the low atmospheric pressure can be calculated with the given voltage-current characteristics of the arcs on pre-contaminated ice surface and in the icicle-icicle air gap and the conductivity of the residual surface on the pre-contaminated ice layer, *i.e.*, parameters  $A_1, B_1, m_1, n_1, e_1, A_2, B_2, m_2, n_2, e_2, A_3, m_3, n_3$ , and  $\gamma_e$ . In our previous studies [27,28], all the parameters were experimentally determined as follows:

Positive arc on pre-contaminated ice-covered ice surface:

$$A_1 = 131.4, B_1 = 756.3, m_1 = 0.81, n_1 = 0.61, e_1 = 0.23$$

Negative arc on pre-contaminated ice-covered ice surface:

$$A_2 = 90.8, B_2 = 500.2, m_2 = 0.74, n_2 = 0.69, e_2 = 0.28$$

Icicle-icicle air gap arc:

$$A_3 = 202.5, m_3 = 0.86, n_3 = 0.53$$

Equivalent surface conductivity of the residual ice layer:

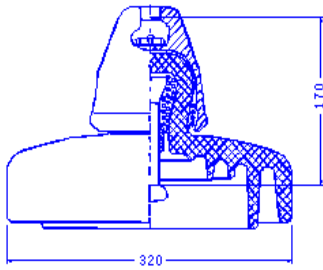
$$\gamma_e = 351.8SDD + 0.091\sigma + 1.9 \quad (\text{under positive arc condition})$$

$$\gamma_e = 345.9SDD + 0.093\sigma + 2.0 \quad (\text{under negative arc condition})$$

where  $SDD$  (in  $\text{mg}/\text{cm}^2$ ) is the salt deposit density of the pre-contaminated insulators, and  $\sigma$  (in  $\mu\text{S}/\text{cm}$ ) is the conductivity of the freezing water (at  $20\text{ }^\circ\text{C}$ ).

To validate the multi-arc model, the model was applied to XZP-210 DC suspension insulators under various conditions. The obtained results were then compared with the experimental ones. Table 1 shows the insulator shape and dimensions.

**Table 1.** Profile Parameters of a Porcelain Insulator.

Type	Dimensions (mm)			Insulator Configuration
	Shed Diameter	Unit Spacing	Leakage Distance	
XZP-210	320	170	545	

The experimental investigations were carried out in the multi-function artificial climate chamber in the High Voltage and Insulation Technological Laboratory of Chongqing University. The artificial climate chamber has a diameter of 7.8 m and a height of 11.6 m. The DC test power supply is a  $\pm 600\text{-kV}/0.5\text{-A}$  cascade rectifying circuit controlled by a thyristor voltage-current feedback system. The technical parameters of the DC test power supply are as follows: the power supply is AC 10 kV, the maximum output voltage is 600 kV, the ripple factor of the test voltage is less than 3% for a current of 500 mA with a resistive load, the relative voltage drop occurring during individual tests resulting in withstand does not exceed 5%, and the relative voltage overshoot due to load-release caused by the extinction of electrical discharges on the insulator surface does not exceed 8%. The measurement accuracy of the resistive potential divider is 0.5%. The negative DC voltage was applied in the tests.

The test procedures are as follows:

(1) **Preparation:** Before the tests, all samples were carefully cleaned to ensure the removal of all traces of dirt and grease. The samples were then naturally dried.

(2) **Artificial pollution:** Insulators may be polluted before icing or during icing. The latter is due to the high water conductivity of the super-cooled water. Accident surveys show that most of the flashovers of the insulator strings of transmission lines in China result from the pollution in the insulators before icing. Rain conductivity is not very high in most mountainous regions in China, and icing often occurs in these areas with a freezing water conductivity of  $80\text{--}120\ \mu\text{S}/\text{cm}$ . Hence, in the current study, the solid layer method was used to form the pollution layer on the samples before ice deposit.

According to IEC 60507 [32], the surfaces of the specimens were contaminated with the suspension of sodium chloride and diatomaceous earth also known as diatomite or kieselguhr, which simulate the electric and inert materials, respectively. In this investigation, the *SDD* were 0.03, 0.05, 0.08, and 0.15 mg/cm<sup>2</sup>, respectively. The ratio of *SDD* to Nonsoluble Deposit Density was 1:6. The contamination layer on the specimens was naturally dried for 24 h.

(3) **Ice deposit:** The specimens were vertically suspended from the hoist at the center of the chamber, rotating at 1 r.p.m. When the temperature in the chamber decreased to  $-7\text{ }^{\circ}\text{C}$ , the surface of the insulators was wetted by the sprayer and covered with a 1–2 mm layer of ice to make sure that the pollution layer would not be cleared away. The spraying system was then used to form wet-grown ice on the insulators without service voltage. To ensure the formation of wet-grown ice on the test insulators, the experimental parameters shown in Table 2 were introduced to this investigation. In such case, the density of the wet-grown ice formed on the composite insulators was about 0.84–0.89 g/cm<sup>3</sup>.

**Table 2.** Experimental parameters of ice deposit.

Droplet ( $\mu\text{m}$ )	Freezing Water Conductivity ( $\mu\text{S}/\text{cm}$ )	Freezing Water Flux ( $\text{L}/\text{h}/\text{m}^2$ )	Air Temperature ( $^{\circ}\text{C}$ )	Wind Velocity ( $\text{m}/\text{s}$ )
80	100	90 *	$-7\sim-5$	3.5 *

\* Except when precise.

The amount of ice accumulated on the insulators could considerably influence their flashover voltages. In this investigation, the average thickness of ice was measured in the applied water exposure zone in a monitoring rotating cylinder with a diameter of 28 mm and rotating at 1 r.p.m. installed near the test insulator. The longitudinal axis was horizontal at each end of the test specimen, so placed to receive the same general wetting as the insulator under test.

(4) **Flashover test:** When the ice thickness reached the target value, flashover tests were carried out on the ice-covered insulators by the up-and-down method according to reference [12] and reference [33] during the melting period. The 50% flashover voltages were obtained. An HG-100K high-speed camera was simultaneously applied to record the whole discharge process during the flashover test to measure the number and lengths of the developing arcs.

The experiment explores the flashover voltages of the 7-unit and 15-unit XZP-210 insulators to validate the rationality of the established model. For the 7-unit XZP-210 insulators, the test conditions are as follows:  $d = 20\text{ mm}$ ,  $SDD = 0.03, 0.05, \text{ and } 0.15\text{ mg}/\text{cm}^2$ ; air pressure  $P = 98.7, 89.8, 79.5, \text{ and } 70.1\text{ kPa}$ ;  $\gamma_e = 100\text{ }\mu\text{S}/\text{cm}$ . Through the discharge route of the arcs filmed by the high-speed camera, the partial arcs are found to usually develop simultaneously from the high voltage end, the ground end, and the part inbetween. The total arc route length varies from 160 to 190 cm, the proportion  $a_1$  of the arc length at the high voltage end ranges from 0.76 to 0.9, and the proportion  $a_2$  of the arc length at the low voltage end is from 0.05 to 0.15. Whether or not the icicle-icicle air gap arc exists is random; if any, there is one or two arcs with  $a_3$  of 0.06–0.15. Therefore, the icicle-icicle air gap arc is chosen as the tested parts to validate the results calculated by the model, as shown in Table 3.

**Table 3.** Test and calculation results of the DC flashover voltage of the ice-covered 7-unit XZP-210 insulator strings.

<i>SDD</i> (mg/cm <sup>2</sup> )	<i>P</i> (kPa)	<i>L</i> (cm)	$\alpha_1$	$\alpha_2$	$\alpha_3$	<i>c</i>	$\sigma$ ( $\mu$ S/cm)	From the Model <i>U<sub>c</sub></i> (kV)	Experimental Results <i>U<sub>f</sub></i> (kV)	$\Delta U\%$
0.03	98.7	166	0.78	0.16	0.06	2	100	87.3	83.3	-4.8
	89.8	185	0.80	0.10	0.10	1	100	89.2	81.1	-10.0
	79.5	185	0.79	0.15	0.06	1	100	70.6	77.2	8.5
	70.1	190	0.90	0	0.10	1	100	66.0	72.6	9.1
0.05	98.7	185	0.80	0.15	0.05	1	100	69.1	75.9	9.0
	89.8	166	0.76	0.09	0.15	2	100	79.2	76.0	-4.2
	79.5	166	0.85	0.05	0.10	1	100	70.7	71.1	0.6
	70.1	185	0.85	0.09	0.06	1	100	59.3	66.0	10.2
0.15	98.7	166	0.80	0.10	0.10	2	100	57.5	60.4	4.8
	89.8	170	0.84	0	0.16	2	100	53.5	59.1	9.5
	79.5	166	0.85	0.05	0.10	2	100	53.4	57.5	7.1
	70.1	166	0.80	0.10	0.10	2	100	50.7	53.0	4.3

For the 15-unit XZP-210 insulators, the test conditions are as follows: ice thickness  $d = 10, 20$  mm;  $SDD = 0.03, 0.05, 0.08,$  and  $0.15$  mg/cm<sup>2</sup>; air pressure  $P = 98.7, 89.8, 79.5,$  and  $70.1$  kPa; and  $\gamma_e = 100$   $\mu$ S/cm. Regardless of the test conditions, the partial arcs usually develop simultaneously from the high voltage end, the ground end, and the part in between. The total arc route length varies from 385–410 cm, the proportion  $\alpha_1$  of the arc length at the high voltage end ranges from 0.74 to 0.81, and the proportion  $\alpha_2$  of the arc length at the low voltage end is from 0.05 to 0.11. The proportion  $\alpha_3$  of the arc length in the middle is within the range of 0.09–0.18. Based on numerous test results, the mean values for the total arc length  $L$ , arc length proportion at the high voltage end  $\alpha_1$ , arc length proportion at the low voltage end  $\alpha_2$ , arc length proportion in between  $\alpha_3$ , and number of icicle-icicle air gap arcs  $c$  are 400 cm, 0.77, 0.08, 0.15, and 4, respectively. These parameters are obtained from the model. The calculation results are compared with the 50% discharge voltage obtained by the test to validate the model, as shown in Table 4.

The following are based on Tables 3 and 4:

(i) For the 7-unit XZP-210 insulator strings, the development characteristics of various types of arcs can be obtained through the discharge process filmed by the high-speed camera. The threshold flashover voltage value calculated by the model established in the current study for the DC discharge of contaminated ice-covered insulators under the low atmospheric pressure is close to the flashover voltage value obtained in the experiments. The maximum comparative error is 10.2%.

(ii) For the 15-unit XZP-210 insulator strings based on one classical type of arc development during the discharge process, the threshold flashover voltage value under different  $SDD$ s, latitudes, and ice thickness conditions calculated by the model established in the current study almost corresponds to 50% flashover voltage value. The comparative error is no more than 10%.

**Table 4.** Test and calculation results of the DC flashover voltage of the ice-covered 15-unit XZP-210 insulator strings.

<i>d</i> (mm)	<i>SDD</i> (mg/cm <sup>2</sup> )	<i>P</i> (kPa)	Experimental Results	From the Model	$\Delta U\%$	
			<i>U</i> <sub>50%</sub> (kV)	<i>U</i> <sub>c</sub> (kV)		
10	0.03	98.7	213.7	225.8	5.7	
		89.8	207.1	215.6	4.1	
		79.5	193.3	203.2	5.1	
		70.1	183.3	191.1	4.2	
	0.05	98.7	201.5	200.1	0.7	
		89.8	194.3	191.1	1.7	
		79.5	182.3	180.8	0.8	
		70.1	173.9	169.3	2.7	
	0.08	98.7	184.6	174.9	5.3	
		89.8	176.5	167.0	5.4	
		79.5	165.0	157.3	4.7	
		70.1	160.2	148.0	7.6	
	0.15	98.7	157.3	148.0	5.9	
		89.8	153.8	141.3	8.1	
		79.5	143.6	133.1	7.3	
		70.1	136.9	125.2	8.6	
	20	0.03	98.7	179.7	182.5	1.5
			89.8	174.9	174.2	0.4
			79.5	164.2	164.1	0.1
			70.1	155.6	154.3	0.8
0.05		98.7	167.8	161.7	3.6	
		89.8	163.2	154.3	5.5	
		79.5	153.0	145.4	5.0	
		70.1	145.9	136.7	6.3	
0.08		98.7	152.4	141.3	7.3	
		89.8	146.6	134.9	8.0	
		79.5	140.5	132.9	5.4	
		70.1	131.8	124.9	5.3	
0.15		98.7	134.5	125.0	7.1	
		89.8	131.7	119.3	9.4	
		79.5	124.2	112.4	9.5	
		70.1	117.7	106.5	9.5	

#### 4. Conclusions

For DC flashover of the pre-contaminated and ice-covered long insulator strings under low air pressure, partial arcs can possibly occur at the high voltage end, the ground end, or between the icicles in the middle part of the insulator string. The coexistence of arcs at several sites and their development until a complete flashover can also occur. The current study developed a DC multi-arc prediction model for the critical flashover voltage of ice-covered long insulator strings under low air pressure. The insulator strings consist of arcs on the ice surface and between icicles based on the Obenaus serial circuit model.

The calculation method of the residual resistance of the ice layer under a DC multi-arc condition was established, which could calculate the residual resistance of the ice surface when there are random numbers of surface arcs and icicle-icicle air gap arcs during the DC discharge process of ice-covered insulator strings.

DC flashover experiments were conducted on 7-unit and 15-unit insulator strings in a multi-function artificial climate chamber. The results show that under the pre-contaminated and low atmospheric pressure conditions, the values calculated by the model correspond to those experimentally measured. The errors were less than 10%, which validates the rationality of the model.

## Acknowledgments

This work was supported by Key Project of Chinese National Programs for Fundamental Research and Development (973 program) (2009CB724502); Project supported by the Funds for Innovative Research Groups of China (51021005); Project Supported by the Fundamental Research Funds for the Central Universities (No. CDJRC10150005).

## References

1. Meier, A.; Niggli, W.M. The Influence of Snow and Ice Deposits on Supertension Transmission Line Insulator Strings with Special Reference to High Altitude Operations. *IEEE Conf. Proc.* **1968**, *44*, 386–395.
2. Cherney, E.A. Flashover performance of artificially contaminated and iced long-rod transmission line insulators. *IEEE Trans. Power Appl. Syst.* **1980**, *PAS-999*, 46–52.
3. Matsuda, H.; Komuro, H.; Takasu, K. Withstand voltage characteristics of insulator strings covered with snow or ice. *IEEE Trans. Power Deliv.* **1991**, *6*, 1243–1250.
4. Farzaneh, M.; Kiernicki, J. Flashover problems caused by ice build-up on insulators. *IEEE Electr. Insul. Mag.* **1995**, *11*, 5–17.
5. Influence of ice and snow on the flashover performance of outdoor insulators Part I: Effects of ice. CIGRE Task Force 33.04.09 Report. *Électra* **1999**, *187*, 90–111.
6. Kannus, K.; Lahti, K. Electrical behaviour of high voltage insulator strings under rime ice. In *Proceedings of the 9th International Workshop on Atmospheric Icing of Structures*, Chester, UK, 5–8 June 2000; p. 8.
7. Jiang, X.L.; Shu, L.C.; Sima, W.X.; Xie, S.J.; Hu, J.L.; Zhang, Z.J. Chinese transmission lines' icing characteristics and analysis of severe ice accidents. *Int. J. Offshore Polar Eng.* **2004**, *14*, 196–201.
8. Fikke, S.M.; Hanssen, J.E.; Rolfseng, L. Long range transported pollution and conductivity on atmospheric ice on insulators. *IEEE Trans. Power Deliv.* **1993**, *8*, 1311–1321.
9. Farzaneh, M.; Kiernicki, J. Flashover problems caused by ice build-up on insulators. *IEEE Electr. Insul. Mag.* **1995**, *11*, 5–17.
10. Farzaneh, M.; Drapeau, J.F. AC flashover performance of insulators covered with artificial ice. *IEEE Trans. Power Deliv.* **1995**, *10*, 1038–1051.
11. Farzaneh, M.; Kiernicki, J. Flashover performance of IEEE standard insulators under ice conditions. *IEEE Trans. Power Deliv.* **1997**, *12*, 1602–1613.

12. Farzaneh, M.; Baker, T.; Bernstorf, A.; Brown, K.; Chisholm, W.A.; de Turreil, C.; Drapeau, J.F.; Fikke, S.; George, J.M.; Gndt, E.; *et al.* Insulator icing test methods and procedures: A position paper prepared by the IEEE task force on insulator icing test methods. *IEEE Trans. Power Deliv.* **2003**, *18*, 1503–1515.
13. Fujimura, T.; Natio, K.; Hasegawa, Y.; Kawaguchi, T. Performance of insulators covered with snow or ice. *IEEE Trans. Power Appl. Syst.* **1979**, *PAS-98*, 1621–1631.
14. Shu, L.C.; Gu, L.G.; Sun, C.X. A Study of Minimum Flashover Voltage of Ice-Covered Suspension Insulators. In *Proceedings of 7th International Workshop on the Atmospheric Icing of Structures*, Chicoutimi, Canada, 3–7 June 1996; pp. 87–92.
15. Jiang, X.L.; Sun, C.X. Study on AC flashover performance and process of ice-covered 10 kV composite insulator. *Proc. CSEE* **2002**, *22*, 58–61.
16. Yi, H.; Wang, L.Q. Measures of preventing ice flashover for transmission line insulator string and analysis of mechanism. *High Volt. Eng.* **2003**, *29*, 57–58.
17. Sun, C.X.; Shu, L.C.; Jiang, X.L.; Sima, W.X.; Gu, L.G. AC/DC flashover performance and its voltage correction of UHV insulators in high altitude and icing and pollution environments. *Proc. CSEE* **2004**, *22*, 115–120.
18. Jiang, X.L.; Wang, S.H.; Zhang, Z.J.; Xie, S.J.; Wang, Y. Study on AC flashover performance and discharge process of polluted and iced IEC standard suspension insulator string. *IEEE Trans. Power Deliv.* **2007**, *22*, 472–480.
19. Hu, J.L.; Sun, C.X.; Jiang, X.L.; Shu, L.C. Flashover performance of pre-contaminated and ice-covered composite insulators to be used in 1000 kV UHV AC transmission lines. *IEEE Trans. Dielectr. Electr. Insul.* **2007**, *14*, 1347–1356.
20. Zhang, J.; Farzaneh, M. Propagation of AC and DC arcs on ice surfaces. *IEEE Trans. Dielectr. Electr. Insul.* **2000**, *7*, 269–276.
21. Farzaneh, M.; Zhang, J.; Chen, X. Modeling of the AC arc discharge on ice surfaces, *IEEE Trans. Power Deliv.* **1997**, *12*, 325–338.
22. Farzaneh, M.; Zhang, J. Modeling of DC arc discharge on ice surfaces. *IEE Proc-C Gener. Transm. Distrib.* **2000**, *147*, 81–86.
23. Farzaneh, M.; Zhang, J. A multi-arc model for predicting ac critical flashover voltage of ice-covered insulators. *IEEE Trans. Dielectr. Electr. Insul.* **2007**, *14*, 1401–1409.
24. Farzaneh, M.; Fofana, I.; Tavakoli, C.; Chen, X. Dynamic modeling of DC arc discharge on ice surfaces. *IEEE Trans. Dielectr. Electr. Insul.* **2003**, *10*, 463–474.
25. Sima, W.X.; Yang, Q.; Sun, C.X.; Guo, F. Potential and electric-field calculation along an ice-covered composite insulator with finite-element method. *IEE Proc-C Gener. Transm. Distrib.* **2006**, *153*, 343–349.
26. Yang, Q.; Sima, W.X.; Sun, C.X.; Shu, L.C.; Hu, Q. Modeling of DC flashover on ice-covered HV insulators based on dynamic electric field analysis. *IEEE Trans. Dielectr. Electr. Insul.* **2007**, *14*, 1418–1426.
27. Hu, J.L. Study on flashover performance and DC discharge model of ice-covered insulator strings at low air pressure. Ph.D. Thesis, Chongqing University, China, 2009; pp. 67–81.
28. Hu, J.L.; Sun, C.X.; Jiang, X.L. Characteristics of surface DC arc on pre-polluted ice and icicle-icicle air gap DC arc under low air pressure. *High Volt. Eng.* **2010**, *36*, 609–615.

29. Farzaneh, M.; Zhang, J.; Chen, X. DC characteristics of local arc on ice surface. *Atmos. Res.* **1998**, *46*, 49–56.
30. Farzaneh, M.; Zhang, J.; Li, Y. Effects of low air pressure on ac and dc arc propagation on ice surface. *IEEE Trans. Dielectr. Electr. Insul.* **2005**, *12*, 60–71.
31. Wilkins, R. Flashover voltage of high-voltage insulators with uniform surface-pollution films. *Proc. IEE* **1969**, *116*, 457–465.
32. International Electrotechnical Commission (IEC). *Artificial Pollution Tests on High-Voltage Insulators to Be Used on A.C. Systems*; Technical Report IEC 60507; IEC: Geneva, Switzerland, 1991.
33. IEEE Dielectrics and Electrical Insulation Society. *IEEE Guide for Test Methods and Procedures to Evaluate the Electrical Performance of Insulators in Freezing Conditions*; IEEE Standard 1783-2009; The Institute of Electrical and Electronics Engineers, Inc.: New York, NY, USA, 2009.

© 2011 by the authors; licensee MDPI, Basel, Switzerland. This article is an open access article distributed under the terms and conditions of the Creative Commons Attribution license (<http://creativecommons.org/licenses/by/3.0/>).